

Characterization of Distance-Dependent Damping in Tapping-Mode Atomic Force Microscopy Force Measurements in Liquid

Ijeoma Nnebe and James W. Schneider*

Department of Chemical Engineering, Carnegie Mellon University,
Pittsburgh, Pennsylvania 15213-3890

Received August 5, 2003. In Final Form: November 18, 2003

We have used a spectral analysis method to characterize changes in the local damping coefficient for an acoustically driven cantilever as it approaches a hard surface in liquid. We show a significant distance dependence of the damping coefficient (and associated quality factor) that must be accounted for to achieve successful theoretical reproduction of experimental tapping-mode force curves. We model the cantilever dynamics using a forced damped harmonic oscillator model and solve the equation of motion using the method of finite differences. Experiments in solutions of differing viscosities show that bulk viscous damping is not the source of the system dissipation, while simulations of the cantilever dynamics including adhesion hysteresis also eliminate this as the origin of the dissipation. We conclude that frictional dissipation that occurs with the intermittent contact is the likely source of dissipation in the system. Our results identify a semiquantitative means of interpreting tapping-mode force curves on nondeformable surfaces in liquid.

Introduction

Tapping-mode atomic force microscopy (TM-AFM)¹ is a widely used tool in the imaging of soft, deformable biological and polymeric surfaces.^{2–5} In this mode of AFM, the cantilever is oscillated at moderate amplitude causing intermittent contact between the tip and surface that minimizes tip–sample contact time and reduces lateral shear of the sample. The cantilever's dynamic response is monitored to provide information about probe–sample interactions and to obtain topographical images and material properties of the surface. In particular, TM-AFM in air has proven invaluable in the imaging of biological molecules such as proteins, DNA, and soft cell surfaces.^{2,6} It is also desirable to image such surfaces under physiological conditions in order to obtain structures of the molecules/surfaces in their natural environment^{7–13} and to measure their intermolecular forces to help uncover

the molecular basis of their function. When using TM-AFM to study these various soft surfaces, it is important to consider all factors that affect the dynamic response of the cantilever. Several modes of energy dissipation exist for TM-AFM in liquid and should be fully characterized for a correct interpretation of both TM-AFM images and force measurements in this medium.

The hydrodynamic damping that affects the free oscillatory motion of AFM cantilevers has been well described theoretically.^{14–16} Here, “free” refers to separation distances at which tip–sample interactions are negligible or, essentially, when the cantilever's oscillations are unaffected by the sample surface. This damping has an inertial component, caused by a mass of liquid that moves with the oscillating cantilever, and a viscous component caused by the resistance of the fluid that must be displaced by the moving lever.¹⁶ Additional drag can also occur due to the squeezing of liquid out of the gap between the cantilever and surface or tip and surface. This drag has been referred to as “squeeze damping”,¹⁷ and its magnitude is dependent on the gap distance between the mean position of the cantilever/tip and the sample surface and the square of the squeeze object size. Theories describing this form of viscous drag predict the cantilever squeeze drag coefficient to scale as D^{-3} ,¹⁸ but experimentally it has been observed to scale as D^{-1} ,^{19,20} where D is the gap distance between the cantilever and sample surface. The “tip squeeze drag coefficient” displays a more sensitive distance dependence at the nanometer scale relevant to TM force measurement and imaging experiments. This damping coefficient is predicted to scale as D^{-1} ¹⁶ and is

* To whom correspondence should be addressed. Telephone: 1 (412) 268-4394. Fax: 1 (412) 268-7139. Electronic mail: schneider@cmu.edu.

(1) Zhong, Q.; Inniss, D.; Kjoller, K.; Elings, V. B. *Surf. Sci. Lett.* **1993**, *290*, L688.

(2) Hansma, H. G.; Revenko, I.; Kim, K.; Laney, D. E. *Nucleic Acids Res.* **1996**, *24*, 713–720.

(3) DeRose, J. A.; Revel, J.-P. *Thin Solid Films* **1998**, *331*, 194–202.

(4) Betley, T. A.; Banaszak Holl, M. M.; Orr, B. G.; Swanson, D. R.; Tomalia, D. A.; Baker, J. R., Jr. *Langmuir* **2001**, *17*, 2768–2773.

(5) Holland, N. B.; Xu, Z.; Vacheethasane, K.; Marchant, R. E. *Macromolecules* **2001**, *34*, 6424–6430.

(6) Vié, V.; Giocondi, M.-C.; Lesniewska, E.; Finot, E.; Goudonnet, J.-P.; Le Grimellec, C. *Ultramicroscopy* **2000**, *82*, 279–288.

(7) Hansma, P. K.; Cleveland, J. P.; Radmacher, M.; Walters, D. A.; Hillner, P. E.; Bezanilla, M.; Fritz, M.; Vie, D.; Hansma, H. G. *Appl. Phys. Lett.* **1994**, *64*, 1738–40.

(8) Putman, C. A. J.; van der Werf, K. O.; De Groot, B. G.; Van Hulst, N. F.; Greve, J. *Appl. Phys. Lett.* **1994**, *64*, 2454–6.

(9) Fritz, M.; Radmacher, M.; Cleveland, J. P.; Allersma, M. W.; Stewart, R. J.; Gieselmann, R.; Janmey, P.; Schmidt, C. F.; Hansma, P. K. *Langmuir* **1995**, *11*, 3529–35.

(10) Hallett, P.; Tskhovrebova, L.; Trinick, J.; Offer, G.; Miles, M. J. *J. Vac. Sci. Technol., B* **1996**, *14*, 1444–1448.

(11) Raab, A.; Han, W.; Badt, D.; Smith-Gill, S. J.; Lindsay, S. M.; Schindler, H.; Hinterdorfer, P. *Nat. Biotechnol.* **1999**, *17*, 902–905.

(12) Osmulski, P. A.; Gaczynska, M. *J. Biol. Chem.* **2000**, *275*, 13171–13174.

(13) Revenko, I.; Proksch, R. *J. Appl. Phys.* **2000**, *87*, 526–533.

(14) Inaba, S.; Akaishi, K.; Mori, T.; Hane, K. *J. Appl. Phys.* **1993**, *73*, 2654–8.

(15) Sader, J. E. *J. Appl. Phys.* **1998**, *84*, 64–76.

(16) O'Shea, S. J.; Welland, M. E. *Langmuir* **1998**, *14*, 4186–4197.

(17) Williams, J. A. *Engineering Tribology*; Oxford University Press: Oxford, New York, Tokyo, 1994.

(18) Hosaka, H.; Itao, K.; Kuroda, S. *Sens. Actuators, A* **1995**, *A49*, 87–95.

(19) Alcaraz, J.; Buscemi, L.; Puig-de-Morales, M.; Colchero, J.; Baro, A.; Navajas, D. *Langmuir* **2002**, *18*, 716–721.

(20) Ma, H.; Jimenez, J.; Rajagopalan, R. *Langmuir* **2000**, *16*, 2254–2261.

commonly three orders of magnitude smaller than the cantilever squeeze-damping coefficient. O'Shea and Welland confirmed this experimentally in their study of solvation forces using noncontact, dynamic AFM, in which they failed to observe tip–surface squeeze damping.¹⁶

Much of the experimental and theoretical work on squeeze damping applies to conditions where the oscillation amplitude is much smaller than D . For TM operation, however, the oscillation amplitude is comparable to D , resulting in the intermittent contact that is the basis of the measurement. Consequently, it is possible that distance-dependent viscous damping is more significant in TM-AFM operation in liquid, since in a single oscillation cycle the squeeze gap can vary from finite distances to zero. Other modes of energy dissipation may be important in TM due to the contact that occurs between the tip and sample. Any strong adhesion between the tip and sample will dissipate energy from the system. Additionally, lateral sliding of the tip during contact because of its off-normal approach to the sample²¹ and buckling of the cantilever due to acoustic waves generated during acoustic excitation²² may promote frictional energy dissipation. In this work, we measure the distance dependence of the energy dissipation experimentally through the cantilever thermal resonance response during TM operation in liquid. We then use these results to quantitatively predict TM-AFM force curves using numerical simulations of the cantilever dynamics.

A few authors have modeled the cantilever dynamics in TM liquid operation with comparison to experiment. In 1996, Chen et al.²² modeled the dynamics of a cantilever tapping on silicon in liquid and used a squeeze-damping theoretical model ($\propto D^{-3}$) to account for the hydrodynamic drag in the system. Though there was fair agreement between their simulation results and the experiment, the shapes of the force curves were quite different, and this was attributed to the limitations associated with using the one-dimensional harmonic oscillator model to describe the movement of the complex three-dimensional cantilever structure. We will show in our work that we can successfully reproduce the shape of our experimental force curve and achieve good agreement using the one-dimensional model when we utilize the distance-dependent damping we measure experimentally. Measurements are made under the same conditions used for conventional TM imaging experiments in liquid, with oscillation amplitudes of 5–10 nm and a driving frequency close to the fundamental cantilever resonance frequency.

Experimental Methods

A Nanoscope III Multimode AFM was used to collect all TM force measurements. In this system, acoustic excitation (forced vibration of the fluid cell) is utilized to promote cantilever oscillation. To collect the resonance spectra of the cantilever, the photodetector signal was streamed at a high frequency (~ 0.5 MHz), amplified using a $10\times$ gain, and stored using a Labview high-frequency data acquisition card simultaneous to force curve collection at a 0.1 Hz ramp rate. This time-domain data was then divided into subsets corresponding to ~ 1 nm spacing, and these subsets were converted to Fourier space with a Hanning window and 69 averages. It was necessary to acoustically drive the cantilever to obtain a self-consistent measure of the quality of resonance.

TM force measurements were conducted on silicon in ultrapure water (MilliQ Gradient A10 System, Millipore) or 50 mM NaCl (Sigma-Aldrich). It was found that addition of salt did not affect

the amplitude changes with separation in the TM force curves. Prior to use, both the silicon surfaces and cantilevers were cleaned for 35 min using UV and ozone irradiation (UVO cleaner, model 42, JeLight, Irvine, CA). V-shaped silicon nitride cantilevers with spring constants of approximately 0.5 N/m were used to conduct the force measurements. Exact values of the spring constants were obtained using the method of Hutter and Bechhoefer.²³ In some experiments, measurements were conducted in water/glycerol (Sigma Aldrich) mixtures of various concentrations to investigate bulk viscosity effects on cantilever dynamics.

Analysis

The motion of the TM cantilever forced to oscillate using a sinusoidal external drive in liquid is modeled using the one-dimensional forced damped harmonic oscillator model. This is only valid under the assumption that the primary mode of vibration is more dominant than secondary vibrational modes. It has been shown that the ratio between the amplitude of the fundamental bending mode and secondary modes decreases in liquid as compared to air; however, the primary mode is still the dominant mode of vibration during tapping.²⁴

Near the surface, tip–sample interactions and viscous damping become significant and will affect the cantilever response. The cantilever dynamics including the effects of tip–sample interaction and the possibility of distance-dependent viscous dissipation can be described using this equation of motion^{25,26}

$$m \frac{d^2x}{dt^2} + \gamma[D] \frac{dx}{dt} + k_c(x - D) = F_{\text{drive}} + F_{\text{P-S}}(x) \quad (1)$$

In the above equation, x is the instantaneous tip position and D is the equilibrium or mean tip–sample separation distance in each oscillation cycle. Both vary with time, t ; however changes in D (mediated through movement of the sample stage toward or away from the oscillating tip) occur much slower than the variation in x . The physical properties of the cantilever are represented through an effective mass m that includes the mass of liquid that oscillates with the lever and the cantilever restoring force/spring constant k_c . External perturbations to the oscillator include the driving force required to sustain oscillation F_{drive} , viscous damping that opposes cantilever acceleration and is characterized by the coefficient γ , and the tip–sample interaction denoted by $F_{\text{P-S}}$.

Equation 1 can be recast in terms of more directly accessible variables experimentally

$$\frac{d^2x}{dt^2} + \frac{\omega_o}{Q[D]} \frac{dx}{dt} + \omega_o^2(x - D) = \omega_o^2[a_d \sin(\omega t)] + \frac{\omega_o^2 F_{\text{P-S}}(x)}{k_c} \quad (2)$$

In eq 2, the substitution $\omega_o = (k_c/m)^{1/2}$ ²⁷ was made to eliminate m from the equation, where ω_o is the resonance frequency of the freely oscillating cantilever with its entrained mass of liquid and ω_o/Q was substituted for the effective damping coefficient, γ/m .²⁷ Q is the quality factor

(23) Hutter, J. L.; Bechhoefer, J. *Rev. Sci. Instrum.* **1993**, *64*, 1868.

(24) Cleveland, J. P.; Anczykowski, B.; Schmid, A. E.; Elings, V. B. *Appl. Phys. Lett.* **1998**, *72*, 2613–2615.

(25) Burnham, N. A.; Behrend, O. P.; Oulevey, F.; Gremaud, G.; Gallo, P.-J.; Gourdon, D.; Dupas, E.; Kulik, A. J.; Pollock, H. M.; Briggs, G. A. D. *Nanotechnology* **1997**, *8*, 67–75.

(26) Chen, J.; Workman, R. K.; Sarid, D.; Höper, R. *Nanotechnology* **1994**, *5*, 199–204.

(27) Fowles, G. R. *Analytical Mechanics*, 4th ed.; Saunders College Publishing: Philadelphia, New York, Chicago, 1986.

(21) Marcus, M. S.; Carpick, R. W.; Sasaki, D. Y.; Eriksson, M. A. *Phys. Rev. Lett.* **2002**, *88*, 226103–1–226103–4.

(22) Chen, G. Y.; Warmack, R. J.; Oden, P. I.; Thundat, T. *J. Vac. Sci. Technol., B* **1996**, *14*, 1313–1317.

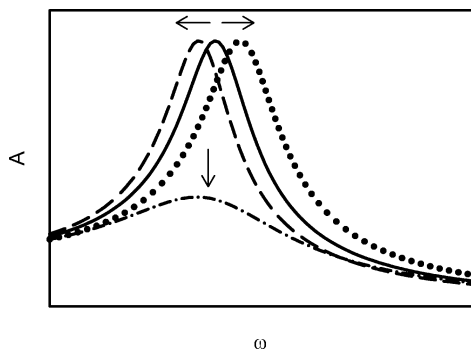


Figure 1. Theoretical resonance curve ($A(\omega)$) of an oscillator when probe–sample interactions are negligible (solid line), the same oscillator perturbed by an attractive probe–sample interaction (dashed line), a repulsive probe–sample interaction (dotted line), and additional damping (dashed–dotted line).

of the lever and is a measure of the sharpness of the resonance response. The driving force is sinusoidal with an amplitude a_d and frequency ω . It is important to note that in either equation we allow the viscous damping to be dependent on D . This deviates from the usual representation of the equation (for operation in air) where the viscous drag component is assumed to be constant and independent of separation.^{25,28,29}

The steady-state solution to eq 2 has been derived using Fourier expansions, assuming sinusoidal tip motion, by Gauthier et al.³⁰ and can be used to determine the oscillation amplitude response as a function of frequency or the resonance response of the cantilever

$$A = \frac{a_d}{\left(1 - \omega^2/\omega_0^2 - r[A]\right)^2 + \frac{\omega^2/\omega_0^2}{Q^2}}^{1/2} \quad (3)$$

There are two significant terms in the equation above that will affect the oscillation amplitude of the cantilever: (i) $r[A]$ the average tip–sample interaction force over an oscillation cycle, scaled by $1/2 k_c A^2$, and (ii) the average viscous damping over an oscillation cycle, represented through Q . Figure 1 depicts how each of the above terms will affect the resonance response of the cantilever. Tip–sample interactions effectively change the spring constant of the system,^{31,32} thereby shifting the frequency at which the maximum amplitude occurs (resonance frequency). Increased viscous drag dissipates energy from the system and, as a consequence, decreases the amplitude of the oscillator.³³ Note that Q is an average of the viscous dissipation over one whole oscillation cycle and it can be affected not only by viscous drag due to the fluid but by viscous losses associated with the tip–sample interaction. The quantity $r[A]$ only represents the conservative part of the tip–sample interaction and is positive for attractive forces and negative for repulsive interactions.

Results and Discussion

Typically in TM force measurements, both the oscillation amplitude of the cantilever and the phase lag in its

(28) Anczykowski, B.; Krueger, D.; Babcock, K. L.; Fuchs, H. *Ultramicroscopy* **1997**, *66*, 251–259.

(29) Bar, G.; Delineau, L.; Brandsch, R.; Ganter, M.; Whangbo, M.-H. *Surf. Sci.* **2000**, *457*, L404–L412.

(30) Gauthier, M.; Tsukada, M. *Phys. Rev. Lett.* **2000**, *85*, 5348–5351.

(31) Anczykowski, B.; Krueger, D.; Fuchs, H. *Phys. Rev. B* **1996**, *53*, 15485–15488.

(32) Bar, G.; Brandsch, R.; Whangbo, M.-H. *Surf. Sci.* **1998**, *411*.

(33) Marion, J. B.; Thornton, S. T. *Classical dynamics of particles and systems*, 3rd ed.; Harcourt Brace Jovanovich: Fort Worth, 1988.

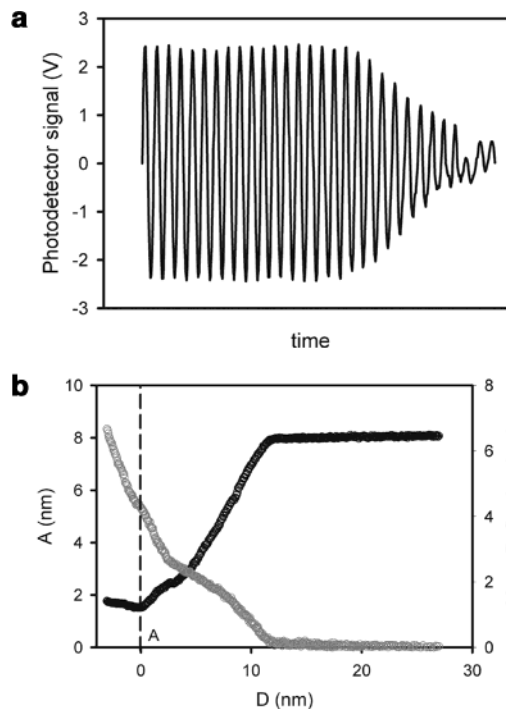


Figure 2. (a) Truncated photodetector signal (amplified V) for a TM force measurement on silicon in water. Number of cycles illustrated was truncated for graphical purposes. (b) Amplitude (black) and mean deflection (gray) versus mean tip–sample separation, D , for the same force measurement. A denotes the defined point of $D = 0$.

response from the drive are used to obtain quantitative measures of the sample material properties and the viscous dissipation in the system. Since most commercial AFMs utilize acoustic excitation to drive the cantilever in liquid, vibration of fluid cell components gives rise to spurious resonances that complicate both the identification of the fundamental resonance frequency of the cantilever and the phase behavior of the cantilever.³⁴ We utilize the resonance frequency obtained from the thermal fluctuations of the cantilever²⁰ to assist in the identification of the fundamental resonance frequency during forced excitation and solely focus on the measurement of oscillation amplitude changes with separation. Figure 2a shows the amplified photodetector signal during a typical force curve on silicon. An important feature of the signal is that the amplitude decays fairly symmetrically. This confirms that the cantilever is being oscillated close to its fundamental resonance frequency.^{8,35}

A well-appreciated complication in interpreting all AFM force curves is the uncertainty associated with the tip–sample separation distance. We have chosen to use the return to constant amplitude (point A in Figure 2b) to calibrate $D = 0$. This return to constant amplitude coincides with a linear increase in the mean deflection of the cantilever (Figure 2b) that we assume is analogous to the linear signal or “constant compliance region” observed in dc AFM. In this constant-compliance region, the tip can no longer approach or indent the sample, and it is the continued linear movement of the sample stage underneath it that causes the linear deflection. We attribute the terminal nonzero amplitude that we observe to the large drive amplitude used to sustain oscillation in acoustic

(34) Schaeffer, T. E.; Cleveland, J. P.; Ohnesorge, F.; Walters, D. A.; Hansma, P. K. *J. Appl. Phys.* **1996**, *80*, 3622–3627.

(35) Lantz, M.; Liu, Y. Z.; Cui, X. D.; Tokumoto, H.; Lindsay, S. M. *Surf. Interface Anal.* **1999**, *27*, 354–360.

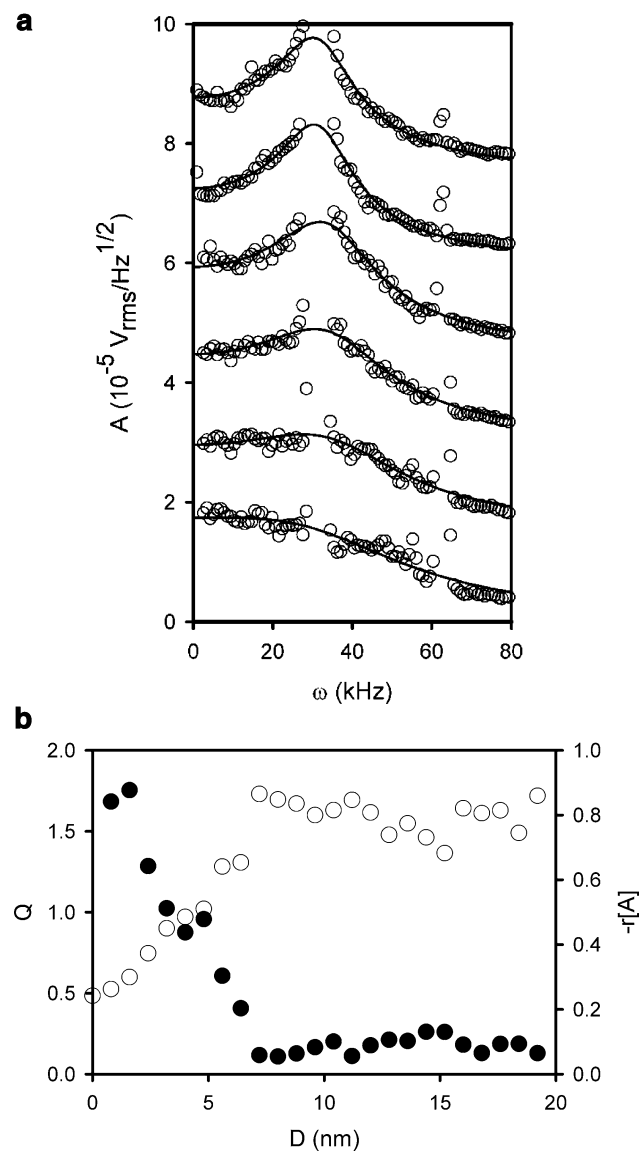


Figure 3. (a) Theoretical fit of $A(\omega)$ curves (eq 3) obtained using Fourier spectroscopy at various D every 0.8 nm from contact ($D = 0$, bottom curve) for a TM force measurement on silicon in water. (b) Fitted Q (white symbols) and $-r[A]$ (black symbols) as a function of D .

liquid operation that causes residual bending of the cantilever.

Fourier transformation of the time domain data in a TM measurement yields spectra consisting of a thermal background and spikes centered at integer multiples of the drive frequency.¹³ These spikes also appear when the laser is reflected off the cantilever substrate, indicating that they are due to the forced translation of the substrate and do not reflect the cantilever dynamics. Therefore, we remove these spikes and fit eq 3 to the broader background thermal peak (Figure 3a). Spectral analyses of the cantilever resonance under driven and non-driven conditions yield identical thermal spectra when the noise spikes are removed.³⁶ Similar observations have been made by Revenko and Proksch¹³ for TM spectra in liquid. As a result, the values of Q obtained by our method are obtained by thermal excitation over a wide range of frequencies, despite the fact that the cantilever is acoustically driven at a nominal drive frequency. Figure 3a shows some of

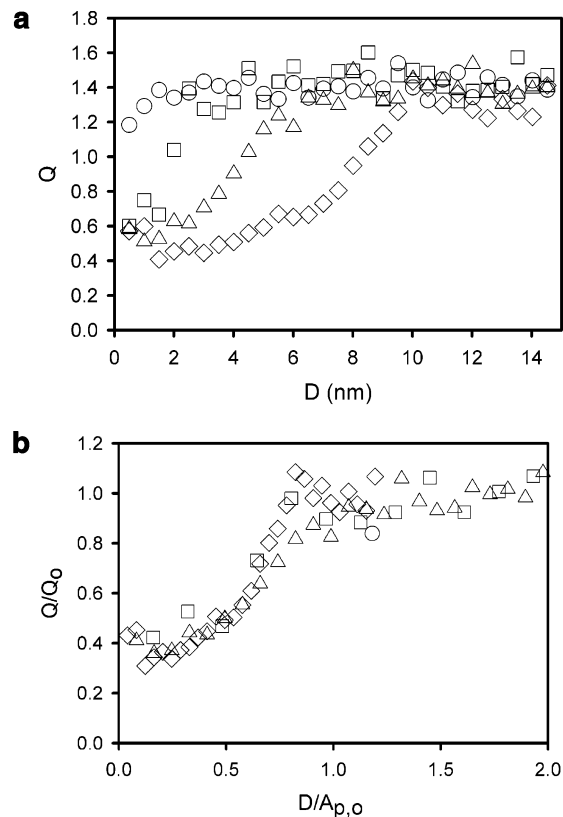


Figure 4. (a) Fitted Q as a function of separation for free peak amplitudes of $A_{p,0} = 0.4$ nm (circles), 3.1 nm (squares), 6.1 nm (triangles), and 12.2 nm (diamonds). (b) Fitted Q as a function of normalized separation, $D/A_{p,0}$, for the data in Figure 4a. Q has also been normalized by its noncontact value.

the fit results. At all separations, the cantilever generally satisfies the harmonic approximation (eq 3). When intermittent contact occurs, there is a large amount of low frequency noise that greatly distorts the resonance spectra below 3 kHz. This is accompanied by higher-order harmonics arising from a distortion of the free cantilever's harmonic potential as the tip contacts the surface. Figure 3b shows the fit parameters Q and $-r[A]$ as a function of separation. $r[A]$ is a negative value due to the dominance of a repulsive tip-sample interaction in the measurement. Q decays significantly once the tip starts to intermittently contact the surface, and $|r[A]|$ increases linearly signifying the growing importance of the repulsive interaction due to contact with the surface.

Bar et al. have shown that the resonance frequency shift is linear with separation when tapping on silicon in air.³² The origin of this linearity is the contact hard wall repulsion that limits the lower turning point of oscillation. When the lower turning point of oscillation is bounded, a symmetric decrease in the upper turning point of oscillation during rebound must occur. This is characteristic of the symmetric vibration of a harmonic oscillator. To determine if the onset of Q decay or increased dissipation was related to the onset of tapping against the silicon sample, we varied the drive amplitude from 5 mV corresponding to a free oscillation peak amplitude, $A_{p,0}$, of 0.4 nm to 100 mV or $A_{p,0} = 12$ nm (Figure 4a). As a point of comparison, the natural thermal fluctuations of this cantilever are about 0.1 nm and do not display any significant change in Q with separation. In Figure 4b, we replot the results by scaling the distance axis by $A_{p,0}$ and normalizing the average interaction by its value at free oscillation. All the curves collapse onto one curve, confirming that the onset of additional dissipation only

(36) Nnebe, I. M.; Schneider, J. W. *Materials Research Society Symposium Proceedings, Volume 790*, Materials Research Society, 2004.

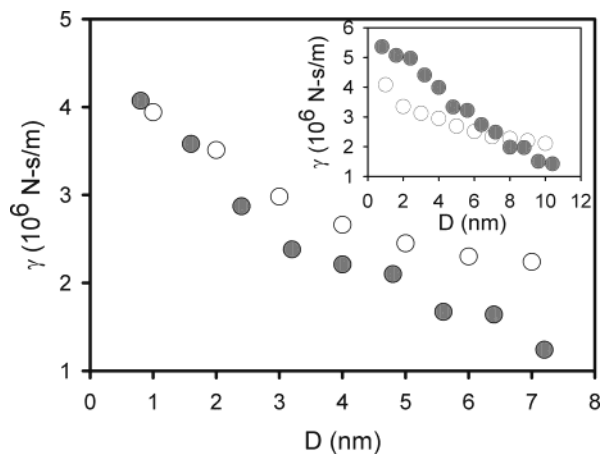


Figure 5. $\gamma(D)$ calculated theoretically (white symbols) and observed experimentally (gray symbols). Inset: $\gamma(D)$ for a larger drive amplitude.

commences with intermittent contact. This is consistent with the constant Q observed when the spectral analysis is conducted for a thermally fluctuating cantilever for which intermittent contact never occurs and suggests bulk viscous effects have no role in the dissipation observed.

We proposed earlier that dissipation due to tip squeeze damping might be more significant in TM than can be described through classical noncontact models such as the Reynolds equation^{16,37}

$$\gamma = 6\pi\eta \frac{R^2}{D} \quad (4)$$

In the above equation, η is the viscosity of the fluid and R is the radius of the hemispherical end of the tip involved in the squeeze damping. We therefore approximate an equivalent γ_{TM} by averaging the computed γ from eq 4 at all tip-sample distances over the oscillation cycle, i.e.

$$\gamma_{\text{TM}} = \frac{\sum_{n=0}^{A_p} \gamma_n}{n} \quad (5)$$

In (5), the constant Q obtained experimentally at noncontact separations was used to calculate an equivalent damping coefficient attributed to cantilever squeeze damping, which was then added to the tip squeeze damping contribution. γ_{TM} calculated using this procedure, assuming $R \sim 28$ nm (the measured tip radius of curvature), results in a $D^{-0.6}$ dependence instead of the D^{-1} dependence usually expected. Additionally, γ_{TM} is about 3 orders of magnitude larger than the conventional tip-squeeze damping calculated for oscillation amplitudes that are much smaller than the gap height. This is due to the cantilever sampling very small separations during its oscillation cycle where large damping is predicted.

Figure 5 shows how the calculated γ_{TM} compares with the experimentally observed damping coefficient, γ_{ex} . No change in γ_{TM} is observed until the onset of intermittent contact; however at this point γ_{ex} displays more sensitive distance dependence than γ_{TM} . This deviation worsens as $A_{p,0}$ increases (inset of Figure 5). We will not place any large significance in the differences observed between γ_{ex} and γ_{TM} because of the simplistic averaging procedure used to obtain γ_{TM} . Instead, to more directly confirm if

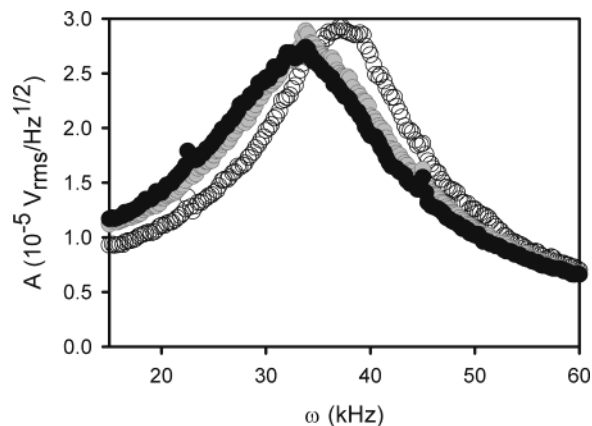


Figure 6. $A(\omega)$ of a free cantilever in water (white symbols); in 10% glycerol (gray symbols); and in 20% glycerol (black symbols).

squeeze damping is the origin of the dissipation we observe during intermittent contact, we conducted more TM force measurements and $A(\omega)$ analysis in aqueous media of different viscosities. The viscosity of water was modified from 1 to ~ 1.4 and ~ 1.85 cP using 10% and 20% glycerol (v/v). The effect of bulk viscosity on the freely oscillating cantilever is best observed in Figure 6, showing resonance spectra obtained from the thermal fluctuations of the cantilever in each of the solutions. As the viscosity of the bulk solution is increased, both the entrained mass of liquid and fluid resistance to displacement increase resulting in a negative frequency shift and broadening of the resonance curve. Figure 7a shows the fitted $Q(D)$ for forced oscillation in all three solutions as a function of separation. The drive amplitude was adjusted in each solution to ensure that the oscillation amplitudes were the same for all the experiments. The viscosity of the solutions affect the cantilever squeeze damping contribution as expected resulting in the different values of Q observed for each solution during the noncontact part of the oscillation. With the onset of intermittent contact, Q decays in all the solutions; however the final Q obtained is independent of the viscosity of the solution. In fact, if we normalize the vertical axis using the free cantilever quality factor Q_0 and again normalize the distance axis using the peak amplitude $A_{p,0}$, all the curves collapse onto each other (Figure 7b), further indicating that the observed dissipation is independent of bulk viscous-drag effects. From eq 4, we expect the damping coefficient due to squeeze flow to be viscosity dependent and therefore we should expect that as we increase the viscosity of the media, the dissipation would increase resulting in lower final Q 's for the solutions of higher viscosity. Since this is not what is observed, we can conclude that squeeze damping is not the origin of the dissipation that is observed experimentally during intermittent contact.

We must therefore consider other possible sources of the energy dissipation. We first investigate the possibility of adhesion hysteresis. To examine this further, we rely on numerical simulations of the cantilever response with separation for three different conditions: (i) constant Q ; (ii) distant-dependent energy dissipation using the Q decay obtained experimentally; and (iii) distant-dependent energy dissipation modeled through adhesion hysteresis. The properties of the cantilever were all measured experimentally, and a Hertzian contact force²⁶ at the silicon surface and an elastic modulus of 180 GPa for the silicon was assumed for cases (i) and (ii). To account for adhesion hysteresis, the Maugis model³⁸ is used with a

(37) Craig, V. S. J.; Neto, C. *Langmuir* **2001**, *17*, 6018–6022.

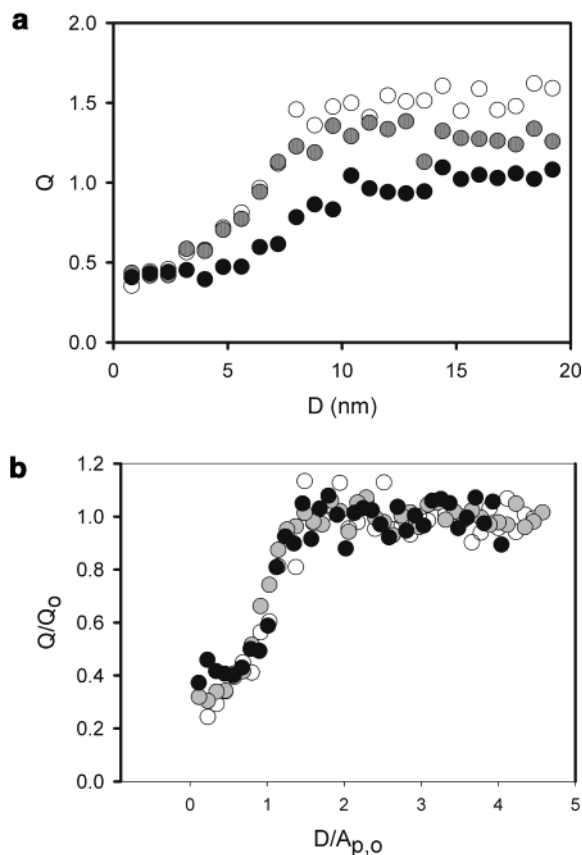


Figure 7. (a) $Q(D)$ for a TM force measurement on silicon in water (white symbols); 10% glycerol (gray symbols); and 20% glycerol (black symbols). (b) Same data except vertical axis has been normalized using the noncontact Q_0 and the horizontal axis normalized using $A_{p,0}$.

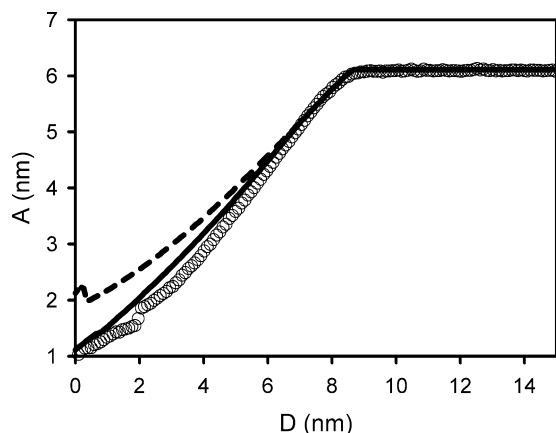


Figure 8. $A(D)$ from a TM force measurement on silicon in water (circles): simulation results using a constant Q (dashed line), and results using the form of Q decay obtained experimentally (solid line).

larger work of adhesion upon retraction away from the surface. The adhesion hysteresis was adjusted until the final oscillation amplitude obtained was the same for the simulation and experiment. The significance of allowing for some form of separation-dependent dissipation is clearly evident through the simulation results (Figure 8). However, when the source of dissipation is modeled as adhesion hysteresis, the shape of the curve is different to that observed experimentally (Figure 9).

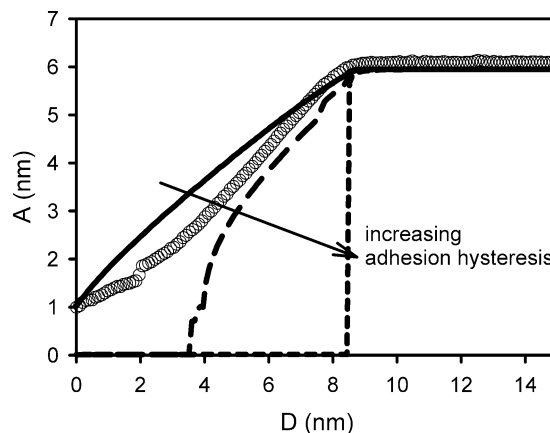


Figure 9. Same experimental data but simulation results now reflect the addition of adhesion hysteresis in the tip-sample interaction. Surface energies during retraction of the tip from the surface were defined as $\varpi_{\text{adh,ret}} = 10 \text{ mJ/m}^2$ (solid line), $\varpi_{\text{adh,ret}} = 20 \text{ mJ/m}^2$ (long dashed line), and $\varpi_{\text{adh,ret}} = 50 \text{ mJ/m}^2$ (short dashed line). Using $\varpi_{\text{adh,ret}} = 50 \text{ mJ/m}^2$, the tip becomes stuck to the surface immediately upon the onset of intermittent contact.

Marcus et al.,²¹ in 1999, identified an important source of dissipation in TM operation that arises from a frictional loss associated with lateral tip motion during contact. This lateral motion is due to the slight inclination of the cantilevers in the fluid cell. Since this dissipation is only associated with contact, it should be independent of the viscosity of the solution but dependent on the material properties of the sample surface. We believe that the dissipation that we have observed has frictional origins that may be due to losses associated with sliding upon contact or/and cantilever buckling suggested by Chen et al.²²

There are some limitations that we must address for the purpose of providing a complete evaluation of the method we have presented. First, it is important to note that though secondary bending modes of the cantilever are not as significant as the primary bending mode, the optical method of detection is still sensitive to these bending modes. This may complicate the identification of local material viscosity with this method where it appears dissipation is friction dominated. Also, since we use the average resonance response to measure dissipation, local sources of dissipation are difficult to identify because the dissipation measured is an average over the entire oscillation cycle spanning distances of a few nanometers. Attempts to quantify local dissipation using smaller amplitudes of oscillation or the thermal fluctuations of the cantilever were unsuccessful, as the large amount of dissipation on contact overdamps the cantilever. Despite these limitations, we have shown that we can obtain good quantitative reproduction of TM force curves in liquid by accounting for distance-dependent damping in the theoretical model of the cantilever dynamics.

Conclusion

We have provided a method for characterizing the dissipation occurring in a TM experiment that will allow external damping effects to be rigorously accounted for in future simulations of the dynamics of the cantilever in TM operation in liquid. We have shown that on silicon, this dissipation is not due to squeeze damping. Instead, the dissipation likely has frictional origins due to sliding of the tip during contact and cantilever buckling caused by the motion of acoustic waves in the system.

We aim to extend our dissipation-characterization method toward TM experiments on compliant surfaces, for which fluid mode TM-AFM is most commonly used. Recent experiments that we have conducted on surfaces bearing grafted polymer have shown that distance-dependence dissipation is also significant in these systems.

Distance-dependent dissipation is significant in TM in liquid and neglecting to account for it can lead to significant inaccuracies in the determination of tip-sample interactions and in topography measurement. We have provided

a useful procedure for quantifying this dissipation with each particular TM measurement.

Acknowledgment. The authors acknowledge the National Science Foundation (CTS-0210205) and the ACS Petroleum Research Fund (#37734-G7) for financial support of this work.

LA030324B